

Landau-Zener-Stueckelberg theory for multiphoton intrashell transitions in Rydberg atoms: Bloch-Siegert shifts and widths

Morten Førre

Laboratoire de Chimie Physique-Matière et Rayonnement, Université Pierre et Marie Curie, 11, rue Pierre et Marie Curie, 75231 Paris Cedex 05, France

(Received 16 July 2003; revised manuscript received 19 December 2003; published 13 July 2004)

We derive closed analytic expressions for intrashell transitions in Rydberg atoms exposed to linearly polarized or circularly polarized periodic electromagnetic fields. The resonance energies and transition probabilities are calculated using multichannel Landau-Zener-Stueckelberg theory. The theory provides formulas for the resonance widths and positions for arbitrary field strength and frequency. The formulas are in excellent agreement with numerical solution of the evolution equations.

DOI: 10.1103/PhysRevA.70.013406

PACS number(s): 32.80.Rm, 33.80.Rv, 33.60.-q

I. INTRODUCTION

The understanding of the interaction of a quantum system with strong periodic fields is the foundation of spectroscopy. In the field of atomic physics, the complex dynamics of a multilevel strongly coupled atom has been and remains a major challenge for experiment and theory. It is of practical importance in both understanding the structure and measuring the excitation modes of the system as well as controlling or engineering the quantum states. The understanding and control of the dynamics of quantum states in a discrete Hilbert space is of great importance in quantum information technology and processing. The development of laser pulses with intensities comparable with internal atomic electric fields, and frequencies in the infrared and ultraviolet spectrum, has led to the observation of highly nonlinear phenomena such as multiphoton ionization and high-order harmonic generation [1]. In the simplest model of nonlinear interaction, the processes can be modeled by an idealized two-level atom [2–4]. This model assumes that the laser-atom coupling is weak enough that only near-resonant transitions will occur, and that selection rules allow us to confine the population transfer between two levels. Then the master equation of the system can be solved in closed analytic form. This provides a physical qualitative understanding of the dynamics and predicts effects such as Rabi oscillations and resonance fluorescence with quantitative precision. The essence of this simplification is the rotating-wave approximation in which the internal and external fields are supposed to be nearly in phase. Counterrotating terms in the Hamiltonian are neglected to a first approximation. The neglect of these nonresonant (virtual) transitions breaks down as the coupling strength increases. Remaining within the framework of the two-state approximation, the corrections that arise from the counterrotating terms are the familiar Bloch-Siegert (BS) shifts [5]. These virtual state corrections are extremely important in precision spectroscopy including photon-atom interactions [6–10], NMR spectroscopy [11–15], electron paramagnetic resonance spectroscopy [16], far-infrared interband transitions in condensed matter [17,18], and continuously driven dissipative solid-state qubits [19].

Metastable Rydberg atoms offer a unique opportunity for accurate studies of pure but strongly driven quantum sys-

tems. The atoms have long lifetimes and very precisely determined energy spectra, and thus have important practical applications in cavity quantum electrodynamics [20] and precise magnetic field measurements [21]. The detailed dynamics of the states within a single manifold, states with a common principal quantum number n , have been studied for single-photon processes, both theoretically and experimentally [21–26]. When intense microwave fields are applied then multiphoton transitions between Rydberg shells can be observed directly [27–29].

In recent high-precision experiments, the Bloch-Siegert shifts and widths of multiphoton resonances in the radio frequency domain were measured [30]. The measurements were of intrashell (same n) transitions of a Rydberg manifold of atomic lithium. Resonances with photon numbers N up to $N=23$ were detected and characterized. Our paper presents closed analytic expressions for the resonance positions and widths corresponding to these measurements. The theoretical model is based on the coherent multichannel Landau-Zener-Stueckelberg model [31–33]. It is explicitly time dependent and general in the sense that it can describe multiphoton absorption dynamics for linear and circular polarization of the oscillating field and arbitrary alignment of an external static electric field. An important advantage of the model is that, as long as intershell mixing can be neglected, the results are valid for strong fields where perturbative methods break down. Our results are in excellent agreement with the observations reported [30].

II. MULTIPHOTON RESONANCES: NUMERICAL SIMULATIONS

The nonrelativistic Hamiltonian of a hydrogenic one-electron atom interacting with a time-dependent electric field can be written as,

$$H = -\frac{1}{2}\nabla^2 - \frac{1}{r} + \mathbf{F}(t) \cdot \mathbf{r}, \quad (1)$$

where \mathbf{F} is the electric field perturbation, and the dipole approximation is made. Atomic units ($\hbar=e=m_e=1$). Suppose that the electron is localized to a single Rydberg manifold n ,

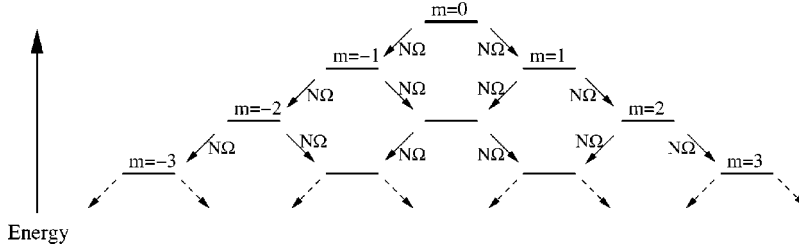


FIG. 1. The energy spectrum of the Stark-split $n=25$ manifold due to a static field F_0 . The energy levels are equidistant and defined with respect to the center of the band by $E_{k,m}=3/2nF_0k$. The nondegenerate initial state $k=n-1, m=0$ is indicated with bold lines in the energy spectrum and the dominant N -photon transitions for circular and linear polarizations are denoted by arrows.

with degeneracy n^2 , and let us take $\mathbf{F}(t)=[F_x \cos \omega t, 0, F_0 + F_z \sin \omega t]$. Thus $F_z=0$ corresponds to linear polarization and $F_z=\pm F_x$ to circular polarization. For perturbations in the presence of a static electric field, the most suitable basis is the set of n^2 orthonormal parabolic states $\{|n, k, m\rangle\}$ where $k=n_1-n_2=-n+|m|+1, -n+|m|+2, \dots, n-|m|-2, n-|m|-1$ is the parabolic quantum number, and $m=-n+1, -n+2, \dots, n-2, n-1$ the projection of the orbital angular momentum along the static field direction. Restricting the Hilbert space to this basis is justified on time scales much shorter than the natural lifetime, and for field strengths such that neighboring Stark n -manifolds do not overlap, that is, $Fn^2 \ll n^{-3}$ [34]. Moreover, only frequencies of the external field ω much lower than the characteristic frequency between neighboring manifolds are considered, that is, $\omega \ll n^{-3}$. In the experiments of interest, carried out by Fregenal *et al.* [30], the parameters were such that $n=25$, $F_0=6$ V/cm, and $0 < (2\pi)^{-1}\omega < 300$, and these conditions were satisfied for all the values of interest.

For a weak field F_0 , the energy shifts of the field-free degenerate manifold are given by the linear Stark effect; $\Delta E_{nkm} = \frac{3}{2}nF_0k$. In Fig. 1 a schematic drawing of the energy levels and the direct transitions between the levels, for $n=25$, are shown. In experimental studies, the state in the n -manifold with largest dipole moment and highest or lowest energy, which is also nondegenerate, can be populated by resonant narrowband excitation from the $2s$ ground state. In the case of interest this corresponds to $|n, k, m\rangle = |25, 24, 0\rangle$. The initial conditions, prior to the application of the oscillatory field, are that this state is fully occupied and the other states are empty. The system can then evolve under the oscillating external field.

An exact one-to-one connection between the dynamics of a single Rydberg manifold perturbed by electromagnetic fields and two independent spin-1/2 systems was established some years ago [35,36] and later generalized to arbitrary initial states [26,37]. The theory has been compared with experiment [21,30] and is now considered to be valid for a large class of problems. Let $c_{k,m}(t)$ be the time-dependent state amplitudes on each Stark state $|n, k, m\rangle$. From this theory the probability of remaining in the initial Stark state $|25, 24, 0\rangle$ with time is given by the simple formula [21]

$$P_{(25,24,0)}(t) = |c_{24,0}(t)|^2 = [1 - p(t)]^{2n-2}, \quad (2)$$

where $p(t)$ is the corresponding transition probability between eigenstates of the coupled two-state system,

$$i \frac{d}{dt} \begin{pmatrix} c_1 \\ c_2 \end{pmatrix} = \begin{pmatrix} H_{11} & H_{12} \\ H_{21} & H_{22} \end{pmatrix} \begin{pmatrix} c_1 \\ c_2 \end{pmatrix}, \quad (3)$$

with $H_{11} = -H_{22} = (3/4)n(F_0 + F_z \sin \omega t)$ and $H_{12} = H_{21} = (3/4)nF_x \cos \omega t$. Prior to the detailed discussion of the physical and analytic aspects of our model, let us consider some results of the numerical integration of these equations. The treelike pairwise coupling of states is shown in Fig. 1. In general, for low-frequency excitations $\omega \ll (3/2)nF_0$, the transitions will be nonresonant and require multiphoton excitation through a sequence of virtual states. This leads to Bloch-Siegert shifts of the energy spectrum characteristic of non-resonant transitions. Suppose that the initial conditions are $c_{24,0}(t=0)=1$ and $c_{k,m}(t=0)=0$ for all other states. We consider the transfer of population from this state due to a short pulse, 10 cycles, of linear or circularly polarized radio-waves in the megahertz region. Results for the probability of remaining in the initial state (adiabatic probability) with respect to variation in the frequency of excitation are shown in Fig. 2. The upper figure indicates the frequency dependence of the probability for linear polarization, while the lower figure considers the example of circular polarization. A regular pattern of resonances corresponding to absorption of a discrete number of photons appears: $N\hbar\omega = E_{nk'm'} - E_{nkm}$, with $N=1, 2, 3, \dots$. Referring to Fig. 2, for the parameters chosen, the low-frequency (higher-order N) transitions are not saturated, while the population is completely depleted for the $N=4$ and $N=3$ transitions after 10 cycles. According to symmetry selection rules [38], the linearly polarized field ($F_z=0$) couples only an odd number of photons, while the circularly polarized field allows both even and odd photon resonances. Furthermore, the position of the resonances is shifted according to the polarization and coupling strength. For example, the $N=5$ resonance is at a higher frequency for linear polarization. Our paper is concerned with a detailed description of these energy shifts. The strength (area of the central maximum) of the resonances decreases rapidly with increasing N . The number of sideband oscillations is proportional to the pulse duration. The relevant experimental parameter is the full width at half maximum FWHM of the resonance envelope rather than the central peak, as indicated in Fig. 3.

III. LANDAU-ZENER-STUECKELBERG MODEL

Recall that the solution to the general problem of intrashell dynamics is exactly described by the evolution of the

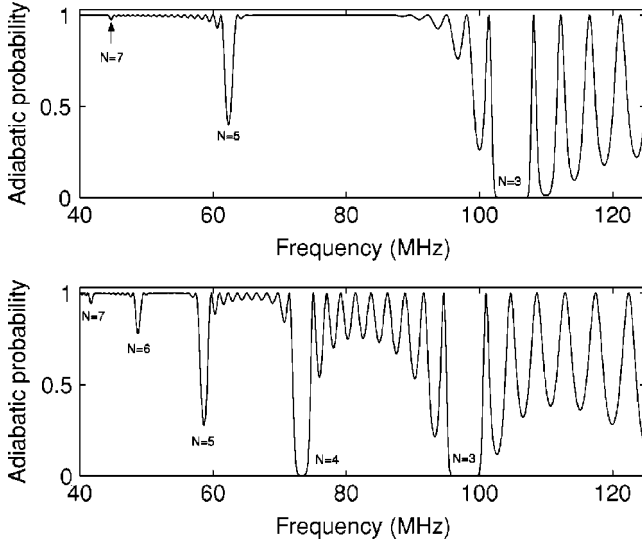


FIG. 2. The probability of the atom remaining in the initial state $|n, k, m\rangle = |25, 24, 0\rangle$ following a 10-cycle pulse of radio frequency radiation in the presence of a static field $F_0 = 6$ V/m. The frequency dependence of the probability is shown for both linear and circular polarizations. Upper figure: results for linear polarization with $F_x = 3.5$ V/cm. Lower figure: results for circular polarization with $F_z = F_x = 1.5$ V/cm. The resonances are labeled by the photon number N corresponding to the energy gap: $\Delta E = N\hbar\omega$.

state amplitudes in the coupled two-level system Eq. (3) [26]. For the Landau-Zener-Stueckelberg [31,39,40] model $H_{11} = -H_{22} = at/2$ while $H_{12} = H_{21}^* = d$. This model is sometimes termed the linear model corresponding to the t dependence of the diagonal energies, and for this Hamiltonian the coupled equations can be solved exactly to yield the transition probabilities between the states. The Landau-Zener-Stueckelberg Hamiltonian has proved to be applicable to a large class of problems and is in many cases the only existing realizable model, due to its simplicity. The amplitudes $c_{1,2}$ are termed the diabatic coefficients because of the crossing $H_{11} = H_{22}$ at $t=0$. We define the unitary (rotation) U such that $a(t) = U(t)c(t)$, so that

$$i\dot{a} = [UHU^\dagger - iU^\dagger\dot{U}]a, \quad (4)$$

with the adiabatic Hamiltonian $H^a = UHU^\dagger - iU^\dagger\dot{U}$. Choosing U to diagonalize H gives: $H_{11}^a = E_1^a(t) = \sqrt{(at/2)^2 + d^2}$ and $H_{22}^a = E_2^a(t) = -E_1^a(t)$. Furthermore, a nonadiabatic coupling $H_{12}^a = H_{21}^{a*} = -iad/(a^2t^2 + 4d^2)$ appears on the off-diagonal elements. The adiabatic transition probability $p = |a_2(+\infty)|^2$ from the initial state $a_i(-\infty) = \delta_{i1}$ is given by the formula [31]

$$p = e^{-2\pi d^2/a}. \quad (5)$$

If a multilevel system exists in which couplings are between pairs of states, and each pseudocrossing is isolated (separated) from the others, then the system can be represented as a series of coupled two-level systems [32,41,42]. However, in applying the two-level formula, one must take proper account of the phase of the coefficient in order to account for interference effects. The S matrix connects the adiabatic am-

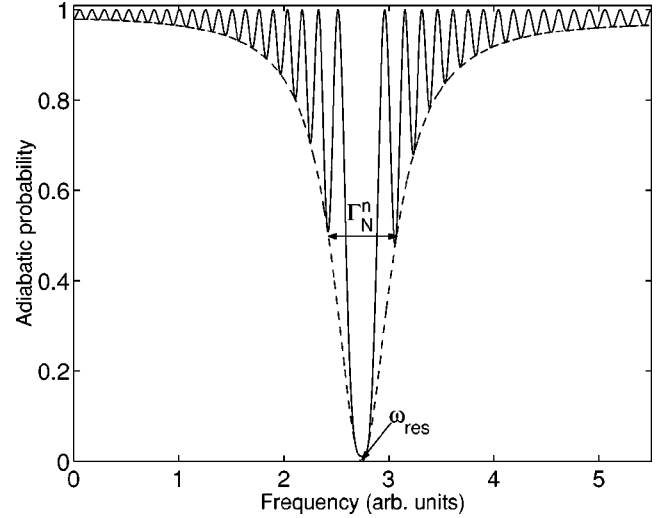


FIG. 3. Definition of the envelope, the width (FWHM), and the resonance frequency of a multiphoton resonance.

plitudes before (τ) and after (τ') the avoided crossing, that is, $a' = Sa$, and it is given by [33]

$$\begin{pmatrix} a_1(\tau') \\ a_2(\tau') \end{pmatrix} = \begin{pmatrix} \sqrt{1-p}e^{-i\Omega'} & -\sqrt{p} \\ \sqrt{p} & \sqrt{1-p}e^{i\Omega'} \end{pmatrix} \begin{pmatrix} a_1(\tau) \\ a_2(\tau) \end{pmatrix}, \quad (6)$$

where $\Omega' = \Omega + \Phi_S$, with Ω the dynamical phase

$$\Omega = \int_{\tau}^{\tau'} |E_{1,2}^a(t)| dt \quad (7)$$

and Φ_S the Stokes phase

$$\Phi_S(a, d) = \frac{\pi}{4} + \frac{d^2}{a} \left(\ln \frac{d^2}{a} - 1 \right) - \arg \Gamma \left(1 + i \frac{d^2}{a} \right). \quad (8)$$

IV. RYDBERG RESONANCES

A. Circular polarization

An in-plane circularly polarized field ($F_z = F_x$) was recently used by Fregenal *et al.* [30] to drive multiphoton intrashell transitions in the radio frequency domain, for highly excited Rydberg atoms. Consider the Hamiltonian in Eq. (3), for $F_z = F_x$, rewritten in the adiabatic basis,

$$H^a = \begin{pmatrix} \frac{\epsilon}{2} \sqrt{1 + \alpha^2 + 2\alpha \sin \omega t} & \frac{i}{2} \frac{\alpha \omega (\alpha + \sin \omega t)}{1 + \alpha^2 + 2\alpha \sin \omega t} \\ -\frac{i}{2} \frac{\alpha \omega (\alpha + \sin \omega t)}{1 + \alpha^2 + 2\alpha \sin \omega t} & -\frac{\epsilon}{2} \sqrt{1 + \alpha^2 + 2\alpha \sin \omega t} \end{pmatrix}, \quad (9)$$

where $\alpha \equiv F_x/F_0$ and $\epsilon \equiv 3nF_0/2$. The adiabatic terms (diagonal elements) now oscillate so that the closest approach of the terms occurs whenever $\sin \omega t = -1$, that is at the following times: $t_c = 3\pi/(2\omega) + 2\pi q/\omega$ ($q=0, 1, 2, \dots$). This is the region where nonadiabatic coupling will be most effective. The adiabatic energy spectrum in Fig. 4 represents a multi-

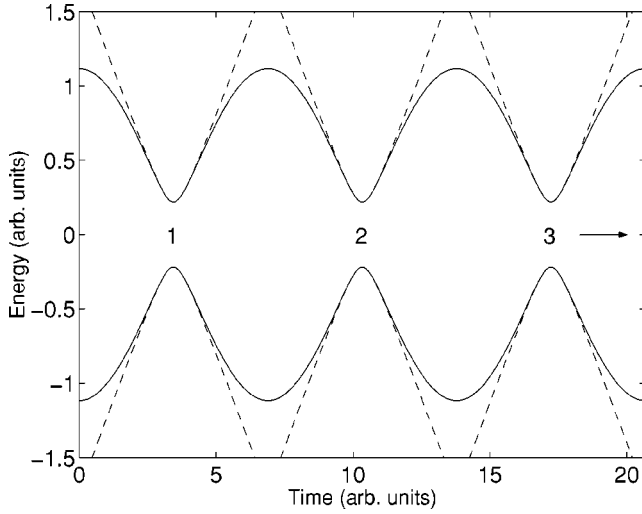


FIG. 4. Typical energy spectrum for the two adiabatic states (full curve), including the three first avoided crossings and the corresponding Landau-Zener-Stueckelberg approximation (dashed curves). The arrows indicates that the spectrum continues periodically in time.

level system with many identical avoided crossings appearing periodically in time. Consider the Taylor expansion of the Hamiltonian near $t \approx t_c$. Comparing with the linear Landau-Zener-Stueckelberg (LZS) model in the adiabatic representation, the following correspondence is clear: $a \equiv \epsilon\omega\sqrt{\alpha}$ and $d \equiv \epsilon(1-\alpha)/2$. The LZS approximation is accurate for $\alpha > 0.2$ and $\omega \ll \epsilon$. Since the transition points t_c are separated by a field period, the isolated two-state model can be used to calculate the depletion of the initial state for each cycle. The final transition matrix after K periods of the field can then be written as a product of totally K S matrices, so that after K cycles (transitions) the probability $P_{ad}(\omega, K)$ of remaining in the initial adiabatic state becomes

$$P_{ad}(\omega, K) = 1 - \frac{1}{4\{1 + [(1-p)/p]\sin^2\Omega'\}} |\lambda_+^K - \lambda_-^K|^2, \quad (10)$$

with

$$\lambda_{\pm} = \sqrt{1-p} \cos \Omega' \pm i\sqrt{p + (1-p)\sin^2\Omega'}.$$

The phase $\Omega' = \Omega + \Phi_S$ is defined by Eqs. (7) and (8). The phase (or action) Ω' generates additional oscillations within the central envelope (see Figs. 2 and 3). In the context of atomic collisions these are usually referred to as Stueckelberg oscillations.

The envelope function $W(\omega)$ has a Lorentz line shape

$$W(\omega) = 1 - \frac{1}{1 + [(1-p)/p]\sin^2\Omega'}, \quad (11)$$

with the line center at $\Omega' = N\pi$ for integer N . Therefore, the resonance frequency is defined by the transcendental equation

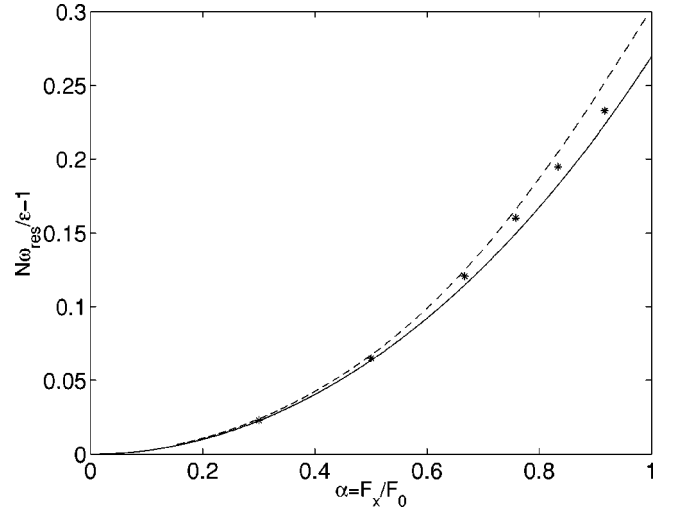


FIG. 5. Variation of scaled Bloch-Siegert shifts $\Delta_{BS} \equiv N\omega_{res}/\epsilon - 1$ with respect to field strength $\alpha = F_x/F_0$ for a circularly polarized field ($F_z = F_x$) and for $N=10$. Analytic results [(Eq. (13)] with $\Phi_S = 0$ (full curve) and $\Phi_S \neq 0$ (dashed curve), respectively. Numerical (exact) results from the direct integration of the coupled equations are indicated by *.

$$\omega = \frac{2\epsilon}{N\pi - \Phi_S(\omega)} (1 + \alpha) E\left(\frac{\pi}{2}, \frac{2\sqrt{\alpha}}{1 + \alpha}\right). \quad (12)$$

Here $E(\pi/2, k)$ is the complete elliptic integral of the second kind [43]. The equation can be solved by iteration to give the simple result

$$\omega_{res} = \frac{\pi\epsilon}{N\pi - \Phi_S(\omega_0)} \left(1 + \frac{1}{4}\alpha^2 + \frac{1}{64}\alpha^4 + O(\alpha^6)\right). \quad (13)$$

We have here assumed that Φ_S is a slowly varying function of ω near the resonance ω_0 , where ω_0 is found from Eq. (13) by putting $\Phi_S = 0$. Note that the Stokes phase can be neglected for large N .

The energy shifts due to the Stokes phase correction can be investigated further. The scaled energy shifts $\Delta_{BS} \equiv N\omega_{res}/\epsilon - 1$ versus scaled harmonic field strength $\alpha = F_x/F_0$ are shown in Fig. 5 for $N=10$. Results for the analytic model with $\Phi_S = 0$ and $\Phi_S \neq 0$ are presented. Since $\Phi_S > 0$, the shifts increase when it is included. The exact result coming from numerical solution of the Schrödinger equation is in close agreement with the analytical estimates.

From Eq. (11), the expression for the full width at half maximum of the resonance corresponding to an N -photon resonance is

$$\Gamma_N = \frac{2\omega_{res}}{N\pi} \sqrt{\frac{p}{1+p}}. \quad (14)$$

Therefore,

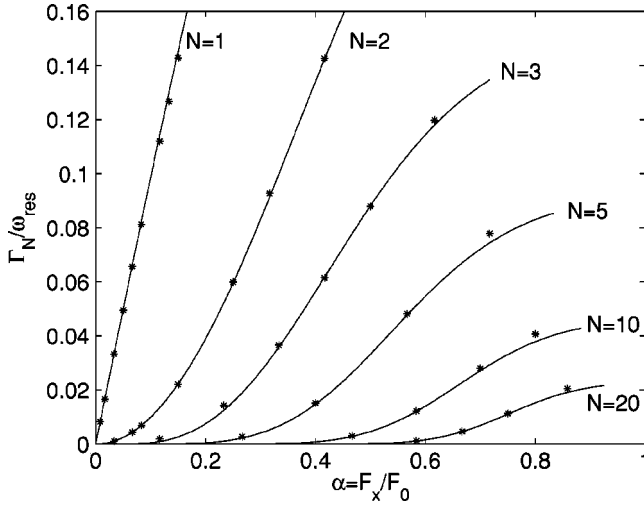


FIG. 6. Widths $\Gamma_N/\omega_{\text{res}}$ (FWHM) (for infinitely long pulse duration) vs scaled harmonic field strength $\alpha = F_x/F_0$ for different photon numbers N , and for a circularly polarized field ($F_z = F_x$). Full curve shows the analytical result [(Eq. (14))] and * the exact numerical results.

$$\Gamma_N \approx \begin{cases} \frac{2\omega_{\text{res}}}{N} \left(\frac{3nF_x}{4\omega_{\text{res}}} \right)^N, & N \leq 2, \\ \frac{2\omega_{\text{res}}}{N\pi} e^{-\pi\epsilon(1-\alpha)^2/4\omega_{\text{res}}\sqrt{\alpha}}, & N > 2, \end{cases} \quad (15)$$

with $p = p(\omega_{\text{res}})$. Since $\epsilon/\omega_{\text{res}} \approx N$ the width is almost independent of the static field F_0 . The widths for $N=1,2$ have been derived by first making the phase transformation $(c_1, c_2) \rightarrow (e^{i3nF_x/(4\omega)\cos\omega t} c'_1, e^{-i3nF_x/(4\omega)\cos\omega t} c'_2)$, to remove the oscillating terms from the diagonal of the coupling matrix in Eq. (3). Keeping only terms involving one- and two-photon resonances, the widths are accurately obtained from perturbation theory [2,44]. The FWHM (Γ_N^n) of a Rydberg resonance is closely related to the two-state width by Eq. (2),

$$\Gamma_N^n = \sqrt{\frac{1}{2^{1/(2n-2)} - 1}} \Gamma_N. \quad (16)$$

In Fig. 6 we have compared the analytical and exact (numerical) widths $\Gamma_N/\omega_{\text{res}}$ for values of N from $N=1-20$. A very high degree of agreement is achieved, illustrating that the analytic formulas Eqs. (14) and (15) are extremely accurate in the range of physical interest $0 \leq \alpha < 1$. In the limit $\alpha \rightarrow 0$, $\Gamma_N \rightarrow 0$, and the lines are sharp for long pulses. However, for a pulse of finite duration ΔT and for $p \ll 1$ the probability that the initial state survives is given by

$$P_{\text{ad}}(\omega, K) = 1 - p(1 - \cos 2K\Omega)/(1 - \cos 2\Omega) + O(p^2),$$

for $\Phi_S = 0$. Since $\lim_{\alpha \rightarrow 0} P_{\text{ad}}(\omega_{\text{res}}, K) = 1 - K^2 p$, then the FWHM becomes

$$\lim_{\alpha \rightarrow 0} \Gamma_N = \frac{4\sqrt{2}}{N\Delta T}. \quad (17)$$

B. Linear polarization

The case with a linearly polarized field ($F_z = 0$) has been widely studied due to its prevalence in optics [2,3,10,45]. In the adiabatic basis,

$$H^a = \begin{pmatrix} \frac{\epsilon}{2} \sqrt{1 + \alpha^2 \cos^2 \omega t} & -\frac{i}{2} \frac{\alpha \omega \sin \omega t}{1 + \alpha^2 \cos^2 \omega t} \\ \frac{i}{2} \frac{\alpha \omega \sin \omega t}{1 + \alpha^2 \cos^2 \omega t} & -\frac{\epsilon}{2} \sqrt{1 + \alpha^2 \cos^2 \omega t} \end{pmatrix}, \quad (18)$$

with $\alpha \equiv F_x/F_0$ and $\epsilon \equiv 3nF_0/2$ as before. Coupling occurs periodically at times $t_c = \pi/(2\omega) + \pi q/\omega$ ($q=0,1,2,\dots$). Accordingly, we have $\sin \omega t \approx \pm 1 \mp \omega^2(t-t_c)^2/2$ and $\cos \omega t \approx \omega(t-t_c)$ near each avoided crossing. Once again the Hamiltonian corresponds to the linear model in the adiabatic representation with the parameters $a = \epsilon\omega\alpha$ and $d = \epsilon/2$. This in turn gives the transition probability p , the Stokes phase Φ_S , and the conditions for resonance. The LZS approximation is accurate for $\alpha \gg 1/\sqrt{2}$ and $\omega \ll \epsilon$. In the weak-coupling limit ($\alpha < 2$) the probability of transition at resonance becomes [2] $p(\omega_{\text{res}}) = 4\pi^2 / \{[(N-1)/2]!\}^4 [3nF_x/(16\omega_{\text{res}})]^{2N}$.

In the strong-coupling region, the probability $P_{\text{ad}}(\omega, K)$ of remaining in the initial state after K rotations of the field has the form

$$P_{\text{ad}}(\omega, K) = 1 - \frac{1}{4\{1 + [(1-p)/p]\cos^2 \Omega'\}} |\lambda_+^K - \lambda_-^K|^2, \quad (19)$$

with

$$\lambda_{\pm} = (1-p)\cos 2\Omega' + p \pm i[4p(1-p)\sin^2 \Omega' + (1-p)^2 \sin^2 2\Omega']^{1/2}.$$

Note that there are two avoided crossings for each period of the field, i.e., totally $2K$ crossings. Hence for finite times ΔT there are twice as many LZS crossings for the linearly polarized field as for the circularly polarized field. From Eq. (19) the envelope function that encloses the resonances becomes

$$W(\omega) = 1 - \frac{1}{1 + [(1-p)/p]\cos^2 \Omega'}. \quad (20)$$

The resonance condition is $\Omega' = N\pi/2$, where N is odd, i.e.,

$$\omega_{\text{res}} = \frac{2\epsilon}{N\pi - 2\Phi_S(\omega_0)} \sqrt{1 + \alpha^2} E\left(\frac{\pi}{2}, \frac{\alpha}{\sqrt{1 + \alpha^2}}\right) = \frac{\pi\epsilon}{N\pi - 2\Phi_S(\omega_0)} \begin{cases} 1 + \frac{1}{4}\alpha^2 - \frac{3}{64}\alpha^4 + O(\alpha^6), & \alpha \leq 1, \\ \frac{2}{\pi}\alpha, & \alpha \geq 1. \end{cases} \quad (21)$$

To second order in α the resonance frequency is similar for

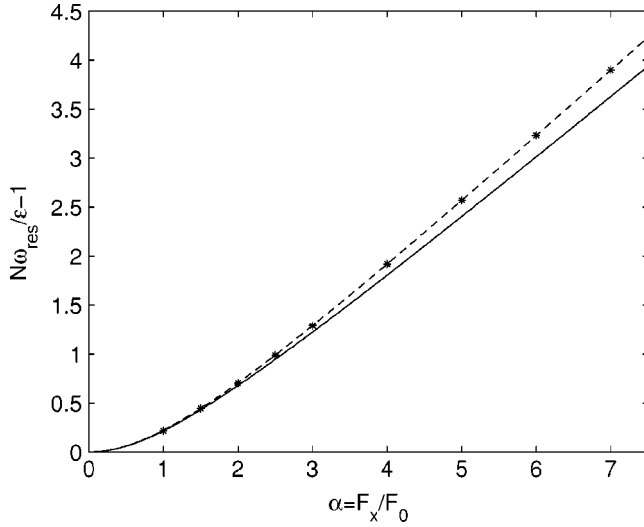


FIG. 7. Same as Fig. 5 for a linearly polarized oscillating field ($F_z=0$) and for $N=7$. Analytical shifts [(Eq. (21)] with $\Phi_S=0$ (full curve) and $\Phi_S \neq 0$ (dashed curve), respectively. Exact numerical shifts shown by *.

the two different polarizations (linear and circular). On the other hand, the fourth-order correction differs in magnitude and sign, from $+1/64\alpha^4$ for circular polarization to $-3/64\alpha^4$ for linear polarization. To check the validity of the resonance formula we have compared it with earlier derivations by Shirley [2], Ahmad and Bullough [46] and Duvall, Valeo, and Oberman [3]. In those derivations the correction Φ_S was not considered. In the limit $N \gg 1$, when Φ_S can be neglected, then our results are in complete agreement. For small values of α the LZS approximation for the Stokes phase is less accurate, and Eq. (21) should be used with caution. In this limit one can set $\Phi_S=0$ since $\lim_{\alpha \rightarrow 0} \Phi_S=0$.

Results for the scaled Bloch-Siegert shift Δ_{BS} versus scaled harmonic field strength $\alpha=F_x/F_0$ are shown in Fig. 7 for $N=7$. The shift becomes significant for strong coupling. However, even for high values of N ($N=7$), the importance of the Stokes phase is clearly visible. Only when this correction is taken into account do we obtain complete agreement between theory and exact numerical calculations. The success for strong coupling reflects the fact that the LZS model is more realistic in this limit. Note that the shift increases linearly with the coupling parameter in the range $\sim 2\alpha/(\pi - 2\Phi_S/N)$ for $\alpha \gg 1$.

Returning to the FWHM of the N -photon resonance, we have that

$$\Gamma_N = \frac{4\omega_{\text{res}}}{N\pi} \sqrt{\frac{p}{1+p}}, \quad (22)$$

so that

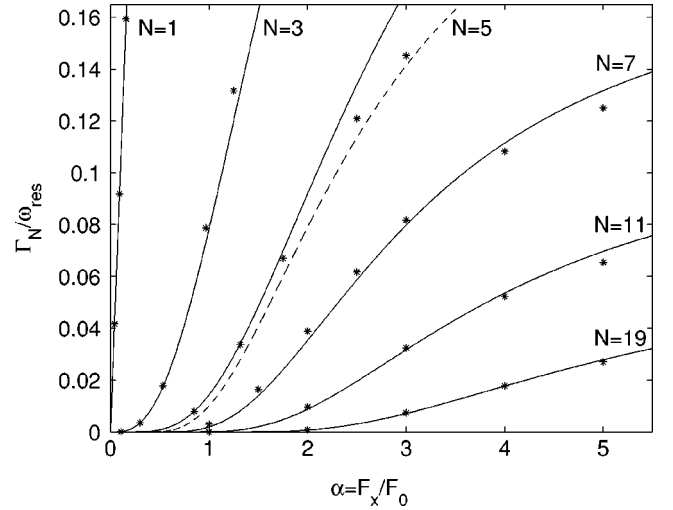


FIG. 8. Same as Fig. 6 for a linearly polarized oscillating field ($F_z=0$). Full curve shows the analytical widths [Eq. (23)] and * the exact numerical widths. For $N=5$ both the formulas valid for $N \leq 5$ (full curve) and $N \geq 5$ (dashed curve), respectively, are shown for comparison.

$$\Gamma_N \approx \begin{cases} \frac{8\omega_{\text{res}}}{N \left[\left(\frac{N-1}{2} \right)! \right]^2} \left(\frac{3nF_x}{16\omega_{\text{res}}} \right)^N, & N \leq 5, \\ \frac{4\omega_{\text{res}}}{N\pi} e^{-\pi\epsilon/4\omega_{\text{res}}\alpha}, & N \geq 5. \end{cases} \quad (23)$$

Note that the choice of approximation defined by the value of N corresponds to $\alpha \sim 2$. Thus the expression in Eq. (23) appropriate to $N \leq 5$ and $N \geq 5$ is equivalent to $\alpha < 2$ and $\alpha > 2$, respectively (see Fig. 8). The upper expression ($N \leq 5$) is based on Shirley's result [2], which deviates significantly from our result for $N \geq 5$. On the other hand, for $N \geq 5$ we obtain complete agreement with Duvall, Valeo, and Oberman [3]. Numerical simulations show that Eqs. (22) and (23) are indeed accurate for all N .

Note that the proportionality factor in Eq. (22) is twice that for circular polarization [Eq. (14)]. This is simply a consequence of the fact that there are twice as many avoided crossings per cycle. Note also that Eq. (11) gives resonances for all integer N , in contrast to the odd N criterion for a linearly polarized field, in agreement with conservation laws for angular momentum [38].

In Fig. 8 the scaled widths $\Gamma_N/\omega_{\text{res}}$ versus scaled harmonic field strength $\alpha=F_x/F_0$ are shown and compared with exact numerical widths for selected values of N . For $N=5$ both formulas valid for $N \leq 5$ and $N \geq 5$ are shown for comparison. Together the two analytical expressions cover all values of N .

Again for a pulse of finite duration ΔT the width approaches the value $4\sqrt{2}/(N\Delta T)$ for $\alpha \rightarrow 0$. This is identical with the result for circular polarization [Eq. (17)]. It follows from the expansion

$$P_{\text{ad}}(\omega, K) = 1 - p(1 - \cos 4K\Omega)/(1 + \cos 2\Omega) + O(p^2)$$

under the condition that $\Phi_S \approx 0$.

V. CONCLUSION

In conclusion, simple analytical formulas for the widths and positions of multiphoton intrashell resonances in hydrogenic atoms are derived and compared with numerical calculations. A very good agreement is achieved. The theoretical results are also in close agreement with recent related experiments [30]. The formulas are valid for arbitrary photon orders, and cover the entire scale of field intensities, ranging from the weak perturbative limit to strong fields. This consistency opens the opportunity for applications in applied multiphoton high-precision technology. The theoretical results may serve as a tool kit for probing limitations and possibilities in photonics and in discrete-variable quan-

tum systems with obvious applications in quantum information.

ACKNOWLEDGMENTS

The author would like to thank the staff at Laboratoire de Chimie Physique-Matière et Rayonnement, Université Pierre et Marie Curie (Paris), for their hospitality and help during the stay there, and V. Boisbourdain, A. Dubois, D. Fregenal, J. P. Hansen, E. Horsdal-Pedersen, L. B. Madsen, A. Maquet, V. N. Ostrovsky, S. Selstø, and R. Taïeb for many useful discussions on the subject. I also want to thank J. F. McCann and J. M. Hansteen for making valuable contributions to the final shaping of this manuscript. This research was supported by NFR, the Research Council of Norway.

-
- [1] M. Gavrilin, in *Atoms in Intense Laser Fields*, edited by M. Gavrilin, Advances in Atomic, Molecular, and Optical Physics Suppl. 1 (Academic Press, San Diego, 1992).
- [2] J. H. Shirley, Phys. Rev. **138**, B979 (1965).
- [3] R. E. Duvall, E. J. Valeo, and C. R. Oberman, Phys. Rev. A **37**, 4685 (1988).
- [4] V. P. Krainov, V. P. Yakovlev, Zh. Eksp. Teor. Fiz. **78**, 2204 (1980) [Sov. Phys. JETP **51**, 1104 (1980)].
- [5] F. Bloch and A. Siegert, Phys. Rev. **57**, 522 (1940).
- [6] Z. Ficek and B. C. Sanders, J. Phys. B **27**, 809 (1994).
- [7] J. P. D. Martin, Phys. Rev. A **57**, 2002 (1998).
- [8] C. Wei, A. S. M. Windsor, and N. B. Manson, J. Phys. B **30**, 4877 (1997).
- [9] A. D. Greentree, C. Wei, and N. B. Manson, Phys. Rev. A **59**, 4083 (1999).
- [10] A. DiPiazza, E. Fiordilino, and M. H. Mittleman, Phys. Rev. A **64**, 013414 (2001).
- [11] M. H. Levitt, *Spin Dynamics: Basics of Nuclear Magnetic Resonance* (John Wiley & Sons, New York, 2001).
- [12] S. A. Vierkotter, J. Magn. Reson., Ser. A **118**, 84 (1996).
- [13] M. Steffen, L. M. K. Vandersypen, and I. L. Chuang, J. Magn. Reson. **146**, 369 (2000).
- [14] S. Zhang and D. G. Gorenstein, Chem. Phys. Lett. **362**, 278 (2002).
- [15] S. Zhang and D. G. Gorenstein, J. Magn. Reson. **132**, 81 (1998).
- [16] I. Gromov and A. Schweiger, J. Magn. Reson. **146**, 110 (2000).
- [17] A. Dargys, J. Phys.: Condens. Matter **12**, L65 (2000).
- [18] A. Dargys, Phys. Status Solidi B **219**, 401 (2000).
- [19] M. C. Goorden and F. K. Wilhelm, Phys. Rev. B **68**, 012508 (2003).
- [20] J. M. Raimond, M. Brune, and S. Haroche, Rev. Mod. Phys. **73**, 565 (2001).
- [21] D. Fregenal, T. Ehrenreich, B. Henningsen, E. Horsdal-Pedersen, L. Nyvang, and V. N. Ostrovsky, Phys. Rev. Lett. **87**, 223001 (2001).
- [22] R. G. Hulet and D. Kleppner, Phys. Rev. Lett. **51**, 1430 (1983); R. Lutwak, J. Holley, P. P. Chang, S. Paine, D. Kleppner, and T. Ducas, Phys. Rev. A **56**, 1443 (1997).
- [23] J. Liang, M. Gross, P. Goy, and S. Haroche, Phys. Rev. A **33**, 4437 (1986); P. Nussenzveig, F. Bernardot, M. Brune, J. Hare, J. M. Raimond, S. Haroche, and W. Gawlik, *ibid.* **48**, 3991 (1993).
- [24] P. Bellomo and C. R. Stroud, Phys. Rev. A **59**, 2139 (1999); J. Chem. Phys. **110**, 7658 (1999).
- [25] V. N. Ostrovsky and E. Horsdal-Pedersen, Phys. Rev. A **67**, 033408 (2003).
- [26] M. Førre, H. M. Nilsen, and J. P. Hansen, Phys. Rev. A **65**, 053409 (2002).
- [27] T. F. Gallagher, *Rydberg Atoms* (Oxford University Press, Oxford, 1994).
- [28] L. A. Bloomfield, R. C. Stoneman, and T. F. Gallagher, Phys. Rev. Lett. **57**, 2512 (1986).
- [29] E. J. Galvez, P. M. Koch, D. Richards, and S. A. Zelazny, Phys. Rev. A **61**, 060101 (2000).
- [30] D. Fregenal, E. Horsdal-Pedersen, L. B. Madsen, M. Førre, J. P. Hansen, and V. N. Ostrovsky, Phys. Rev. A **69**, 031401(R) (2004).
- [31] C. Zener, Proc. R. Soc. London, Ser. A **137**, 696 (1932).
- [32] D. A. Harmin and P. N. Price, Phys. Rev. A **49**, 1933 (1994); D. A. Harmin, *ibid.* **56**, 232 (1997).
- [33] E. E. Nikitin and S. Y. Umanskii, *Theory of Slow Atomic Collisions* (Springer, Berlin, 1984).
- [34] Y. N. Demkov, V. N. Ostrovsky, and E. A. Solov'ev, Zh. Eksp. Teor. Fiz. **66**, 125 (1974) [Sov. Phys. JETP **39**, 57 (1974)].
- [35] A. K. Kazansky and V. N. Ostrovsky, J. Phys. B **29**, L855 (1996).
- [36] N. V. Vitanov and K. A. Suominen, Phys. Rev. A **56**, R4377 (1997).
- [37] A. K. Kazansky, H. Nakamura, and V. N. Ostrovsky, Laser Phys. **7**, 773 (1997).
- [38] H. M. Nilsen, L. B. Madsen, and J. P. Hansen, J. Phys. B **35**, 403 (2002).
- [39] L. Landau, Phys. Z. Sowjetunion **2**, 46 (1932).
- [40] E. C. G. Stueckelberg, Helv. Phys. Acta **5**, 369 (1932).
- [41] F. Robicheaux, C. Wesdorp, and L. D. Noordam, Phys. Rev. A **62**, 043404 (2000).
- [42] M. Førre and J. P. Hansen, Phys. Rev. A **67**, 053402 (2003).
- [43] I. S. Gradshteyn and I. M. Ryzhik, *Table of Integrals, Series, and Products* (Academic Press, New York, 1994).
- [44] N. Rosen and C. Zener, Phys. Rev. **40**, 502 (1932).
- [45] L. Allen and J. H. Eberly, *Optical Resonance and Two-Level Atoms* (Dover, New York, 1987).
- [46] F. Ahmad and R. K. Bullough, J. Phys. B **7**, 275 (1974).